Conformational Effects on the *pro-S* Hydrogen Abstraction Reaction in Cyclooxygenase-1: An Integrated QM/MM and MD Study

Christo Z. Christov,[†‡]* Alessio Lodola,[§] Tatyana G. Karabencheva-Christova,[†‡] Shunzhou Wan,[¶] Peter V. Coveney,[¶] and Adrian J. Mulholland[†]*

[†]Centre for Computational Chemistry, School of Chemistry, University of Bristol, Bristol, UK; [‡]Department of Applied Sciences, Faculty of Health and Life Sciences, Northumbria University, Newcastle, UK; [§]Dipartimento di Farmacia, Università degli Studi di Parma, Parma, Italy; [¶]Centre for Computational Science, Chemistry Department, University College of London, London, UK

Submitted October 28, 2012, and accepted January 24, 2013.

*Correspondence:Adrian.Mulholland@bristol.ac.uk or Christo.Christov@northumbria.ac.uk

SUPPORTING INFORMATION

STOCHASTIC BOUNDARY MOLECULAR DYNAMICS

The structure of the complex between COX-1 and arachidonic acid was taken from PDB (1diy.pdb) [S1]. CHARMM code (version 27b2) was used for all structure manipulation and calculations [S2]. We selected and kept in the system all protein residues with at least one atom within 25 Å of the center (H13 of COX-1) while all the rest were deleted. The salvation of the system was done by superimposing a 60 Å edge pre-equilibrated box of 8000 TIP3P water molecules [S3]. Any water molecules with oxygen atom within 2.6 Å distance of another non-hydrogen atom were deleted. First, 10 ps of Langevin dynamics [S4] at a temperature of 300 K was performed to equilibrate the water molecules, whilst all other atoms were kept fixed. Then Stochastic Boundary MD simulations were carried out as follows: We defined a 4 Å buffer zone which includes all atoms further than 21 Å away from the center. The non-solvent heavy atoms were restrained to their coordinates by harmonic potentials with force constants based on model average *B*-factors [S5]. These restraints were linearly scaled in four steps, strating from zero at 21 Å from the center of the system, to a maximum value at 25 Å. Langevin dynamics with frictional coefficients of 250 ps^{-1} for non-hydrogen protein atoms and 62 ps^{-1} on water oxygen atoms were applied for the entire buffer region. In addition for the water oxygen atoms were applied deformable boundary potential. CHARMM22 force field (CHARMM22 protein parameters and CHARMM27 lipid parameters [S6] was used. A cutoff distance for non bonded interactions of 13 Å was applied. The simulation was performed at two phases with timestep of 0.5ps: A heating phase in order to increase the temperature from 0 to 300 K was run for 30ps; (*ii*) an equilibration phase at 300 K was performed for 250 ps. The final was MM minimized to an energy gradient of 0.01 kcal mol^{-1} $Å^{-1}$ with the ABNR method before the QM/MM calculations.

PERIODIC BOUNDARY MOLECULAR DYNAMICS

The structure of the enzyme-substrate complex has been taken from Protein Data Bank (PDB id: 1DIY) [S1] and represents a complex of COX-1 with arachidonic acid (AA) in productive orientation and co-substituted heme. The system preparation and simulation have been described in our previous publication [S7]. Here we only briefly summarize the preparation and simulation process.

The CHARMM package [S2] was used for preparing the initial molecular model and analyzing the final results. The CHARMM22 force field [S6] was used throughout. COX-1 was rotated to align its two-fold dimer axis parallel to the membrane normal, and its membrane binding domain (MBD) was embedded into the upper leaflet of a DMPC-based lipid bilayer. The protein-membrane system was carefully constructed, as described in our previous publication [S7]. The upper planes were located at the peaks of the profiles for the cross-sectional area of the MBD along the two-fold dimer axis; the lower planes were 34Å below. The distance corresponds to the head-to-head distance of the DMPC bilayer. The complex was then solvated using TIP3P water molecules [S3] and electrostatically neutralized by adding counterions (Na^+). The final system contained a COX-1 dimer complexed with arachidonic acids and hemes, and 170 and 205 DMPC molecules in the upper and lower layers respectively.

Three-dimensional periodic boundary conditions were applied in the simulation. The minimization and production runs were performed using NAMD [S8]. The electrostatic interaction was divided into two parts: a local component which was calculated every time step with a local interaction distance of 12 Å, and a long-range component which was evaluated every four time steps. Particle mesh Ewald (PME) [S9] was used for the full electrostatic calculations. The vdW interactions were truncated using the switch method with a switch range of 10 – 12 Å. Hydrogen to heavy atom bonds, and the internal geometry of the water molecules, were constrained using SHAKE algorithm [S10] and the equations of motion were integrated with a 2 fs time step. Energy minimizations were first performed with heavy protein atoms restrained at their x-ray positions. Then a series of short simulations were conducted, while the restraints on heavy atoms were gradually reduced. This was followed by free dynamics simulation, assigning random velocities based on a Maxwellian distribution at 100 K as the initial temperature. The systems were heated to the final temperature of 300 K by periodically reassigning the velocities. Finally 25 ns production simulation was run at a temperature of 300 K and a pressure of 1 bar (NPT ensemble). Trajectory coordinates were recorded at every 2 ps.

SELECTIONS OF INITIAL STRUCTURES FOR QM/MM MODELLING

Representative structures were determined by a cluster analysis of the AA conformations [S7]. Most of the “conformational states” [S7]were unlikely to represent a productive binding mode as the distance between *pro-S* hydrogen atom and phenoxyl radical oxygen ([O-H_s] distance) was too great (see Table 2 in reference [S7]. This is not surprising as the representative structures observed in a classical MD simulation are not necessarily the optimal states in quantum calculations. Therefore, the frames were chosen based on the [O-H_s] distance, with a threshold of 3.0Å, instead of using representative structures from MD simulation. They are at least 300ps apart to make them less correlated. The frames differ not only at the [O-H_s] distance,

but the conformations of both protein and arachidonic acid (Figure S1). The conformations were MM and QM/MM minimized before further simulations.

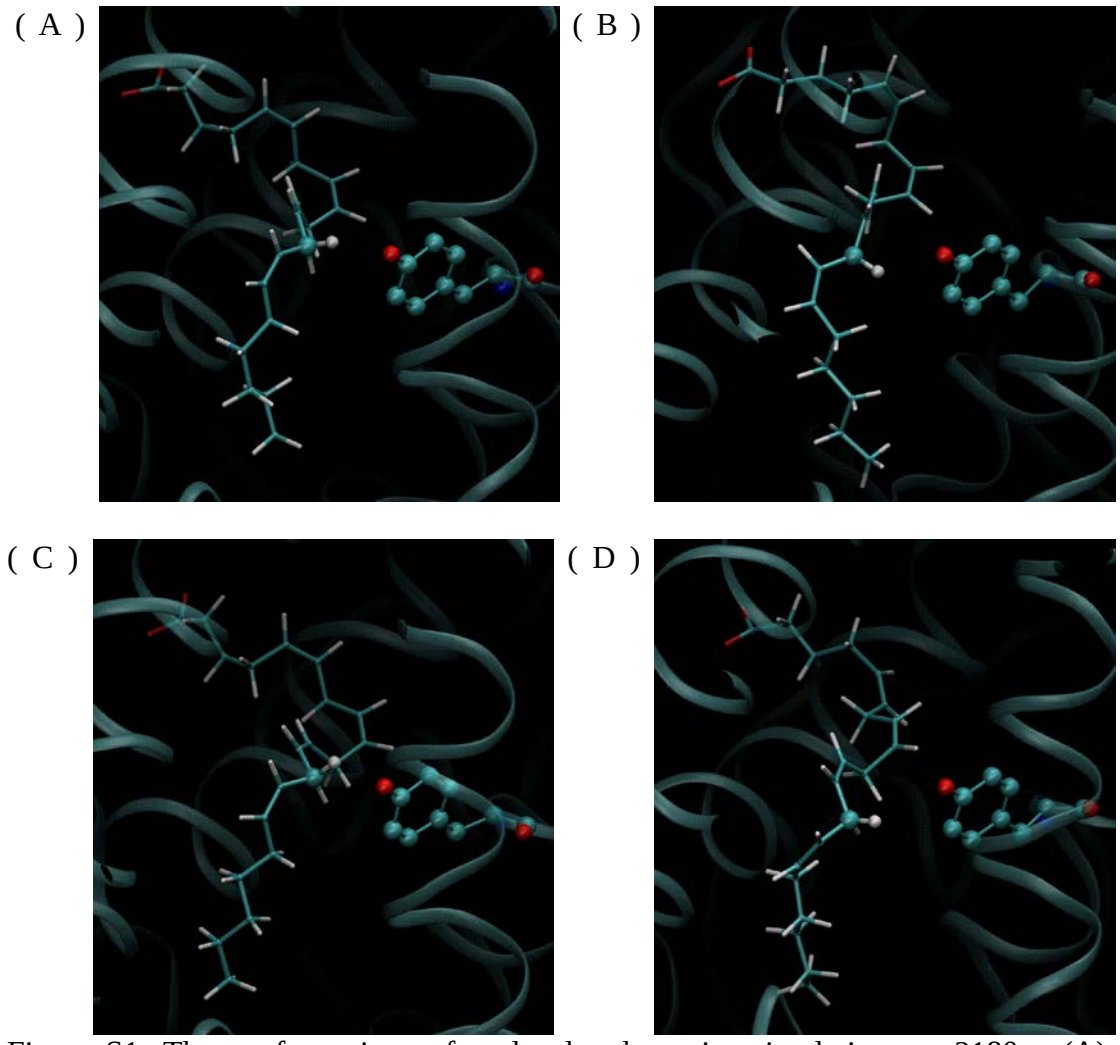

Figure S1. The conformations of molecular dynamics simulations at 2180ps (A), 3984ps (B), 4960ps (C) and 5344ps (D). COX-1 is depicted in ribbon representation, the arachidonic acid in bond model with C13 and *pro-S* hydrogen atoms in ball model, and the residue TYR 385 in ball-and-stick model. The structures are aligned using the sidechain of the TYR 385 residue.

QM/MM METHODOLY

One (hydrogen) 'link atom' was used at the QM/MM boundary, connecting the CB and CA atoms of the tyrosine radical. The QM part (68 atoms) was modelled at the B3LYP/6-31+G(d) level of theory. This method has been shown to perform well for this system [S11, S12]. As the QM part contains an unpaired electron, open shell calculations using Jaguar [S13] were performed. The rest of the system was treated with the CHARMM27 force field [S6] using the TINKER program [S14]. Coupling between the QM and MM regions was done with QoMMMa interface [S15]. All atoms situated outside a 20 Å sphere centred on the C13 atom of ACD were held fixed. The electrostatic interactions between QM and MM regions were accounted for by incorporating the MM atomic charges in the QM Hamiltonian. QM/MM van der Waals interactions were calculated classically by assigning Leonard-Jones parameters

to the QM atoms. No cut-offs for electrostatic and van der Waals interactions were used. All initial structures were QM/MM minimized to within an energy gradient of 0.01 kcal mol^{-1} $Å^{-1}$. The adiabatic mapping (coordinate driving) approach [S16] was used to explore the reaction path for the abstraction of the *pro-(S)*-hydrogen (Hs) from the C13 atom of ACD by the oxygen of the Tyr385 radical. During the adiabatic mapping its value was incremented by 0.2 Å each step, apart from in the proximity of the approximate transition state, where the increment was 0.1 Å. A force constant of 1000 kcal mol^{-1} $Å^{-2}$ was used to restrain the reaction coordinate to each particular value. Energy minimizations at each value of the reaction coordinate were performed to within an energy gradient value of 0.01 kcal mol^{-1} $Å^{-1}$. The structures of energy minima (reactants and products) were determined more precisely by performing additional geometry optimizations with no reaction coordinate restraint.

REFERENCE

S1. Malkowski, M. G., S. L. Ginell, W. L. Smith, and R. M. Garavito. 2000. The productive conformation of arachidonic acid bound to prostaglandin synthase. *Science* 289:1933-1937.

S2. Brooks BR, Bruccoleri RE, Olafson BD, States DJ, Swaminathan S, M K. 1983. CHARMM: A Program for Macromolecular Energy, Minimization, and Dynamics Calculations. *J. Comp. Chem* 4:187-217.

S3. Jorgensen, W. L., J. Chandrasekhar, J. D. Madura, R. W. Impey, and M. L. Klein. 1983. Comparison of Simple Potential Functions for Simulating Liquid Water. *J. Chem. Phys.* 79:926-935.

S4. Brooks, C. L., and M. Karplus. 1989. Solvent effects on protein motion and protein effects on solvent motion. Dynamics of the active site region of lysozyme *J. Mol. Biol.* 208: 159-181

S5. Mulholland, A. J., and W.G. Richards. 1997. Acetyl-CoA enolization in citrate synthase: a quantum mechanical/molecular mechanical (QM/MM) study. *Proteins.* 27:9-25

S6. A. D. MacKerell, Jr., D. Bashford, M. Bellott, R. L. Dunbrack, Jr., J. D. Evanseck, M. J. Field, S. Fischer, J. Gao, H. Guo, S. Ha, D. Joseph-McCarthy, L. Kuchnir, K. Kuczera, F. T. K. Lau, C. Mattos, S. Michnick, T. Ngo, D. T. Nguyen, B. Prodhom, W. E. Reiher, III, B. Roux, M. Schlenkrich, J. C. Smith, R. Stote, J. Straub, M. Watanabe, J. Wiórkiewicz-Kuczera, D. Yin and M. Karplus, 1998. All-atom empirical potential for molecular modeling and dynamics studies of proteins. *J. Phys. Chem B* 102(18):3586-3616.

S7. Wan, S. Z., and P. V. Coveney. 2009. A Comparative Study of the COX-1 and COX-2 Isozymes Bound to Lipid Membranes. *J. Comp. Chem.* 30:1038-1050.

S8. Phillips, J. C., R. Braun, W. Wang, J. Gumbart, E. Tajkhorshid, E. Villa, C. Chipot, R. D. Skeel, L. Kale, and K. Schulten. 2005. Scalable molecular dynamics with NAMD. *J. Comp. Chem.* 26:1781-1802.

S9. Toukmaji, A. Y., and J. A. Board. 1996. Ewald summation techniques in perspective: A survey. *Comp. Phys. Comm.* 95:73-92.

S10. Ryckaert, J. P., G. Ciccotti, and H. J. C. Berendsen. 1977. Numerical-Integration of Cartesian Equations of Motion of A System with Constraints - Molecular-Dynamics of N-Alkanes. *J. Comp. Phys.* 23:327-341.

S11. Blomberg, L. M., Blomberg, M. R. A., Siegbahn, P. E. M., van der Donk, W. A. & Tsai, A. L. (2003) A quantum chemical study of the synthesis of prostaglandin

G(2) by the cyclooxygenase active site in prostaglandin endoperoxide H synthase 1, *Journal of Phys. Chem. B. 107*, 3297-3308.
S12. Silva, P. J., Fernandes, P. A. & Ramos, M. J. (2003) A theoretical study of radical-only and combined radical/carbocationic mechanisms of arachidonic acid cyclooxygenation by prostaglandin H synthase, *Theor. Chem. Acc. 110*, 345-351.
S13. (2005) Jaguar in, Schrödinger, LLC, NY,
S14. Ren, P. Y. & Ponder, J. W. (2003) Polarizable atomic multipole water model for molecular mechanics simulation, *Journal of Phys. Chem. B. 107*, 5933-5947.
S15. Harvey, J. N. (2004) Spin-forbidden CO ligand recombination in myoglobin, *Faradey Discuss. 127*, 165-177.
S16. McCammon, J. A. & Harvey, S. C. (1987) *Dynamics of protein and nucleic acids*, Cambridge University Press, New York.

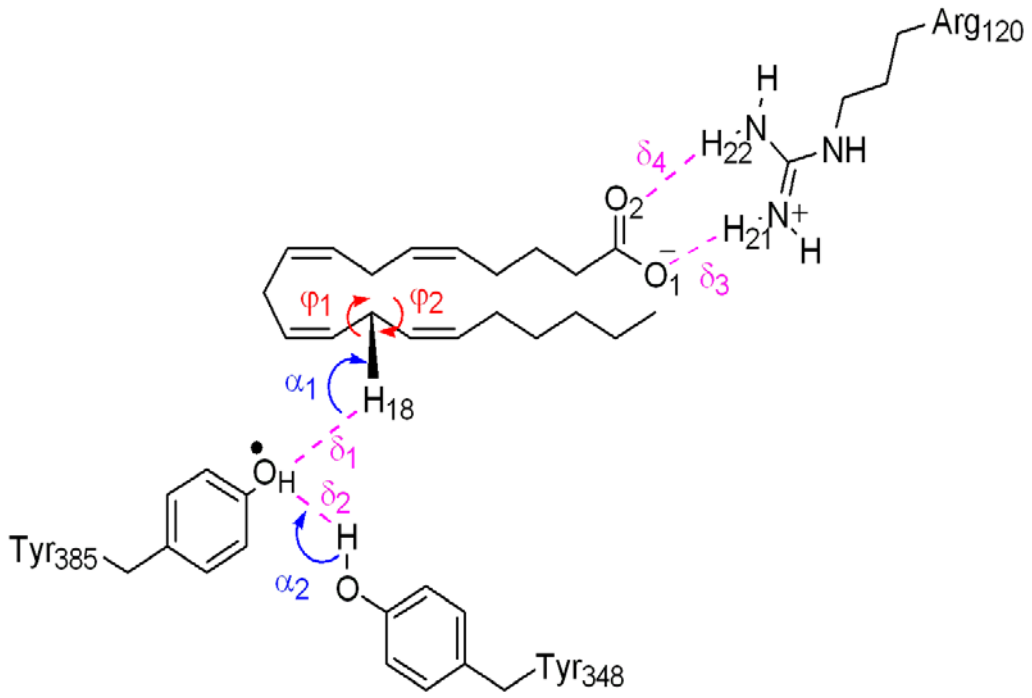

Figure S2. Geometric parameters representing important interactions in COX-1 Michaelis complex.

Structure	$\Delta E^{\#}$	Distance δ_1	Angle α_1	Torsion Angle φ_1	Torsion Angle φ_2	Distance δ_3	Distance δ_4	Torsion Angle φ_3	Distance δ_2	Angle α_2	Torsion Angle φ_4
SBMD	19.00	2.37	108.96	145.51	-141.51	1.63	1.68	-24.50	1.77	174.80	-107.79
4960ps	16.40	2.36	89.26	152.21	-139.84	1.65	1.69	112.40	1.81	172.11	-25.10
2180ps	18.20	2.38	95.18	173.77	-113.48	1.77	1.70	-49.92	1.81	168.51	-16.34
5344ps	14.30	2.48	83.41	142.42	-157.30	1.76	1.64	107.30	1.79	173.65	-45.76
3984ps	25.90	2.44	107.17	96.84	-135.20	1.65	1.63	-51.47	1.98	167.98	-71.81

Table S1 Geometric parameters of Reactant Complex. Distances are presented in [Å], angles and torsion angles in [°].

Structure	$\Delta E^{\#}$	Distance δ_1	Angle α_1	Torsion Angle φ_1	Torsion Angle φ_2	Distance δ_3	Distance δ_4	Torsion Angle φ_3	Distance δ_2	Angle α_2	Torsion Angle φ_4
SBMD	19.00	1.37	110.24	146.94	-151.54	1.63	1.69	-23.96	2.03	172.17	-119.56
4960ps	16.40	1.29	108.43	156.32	-137.61	1.65	1.69	45.22	1.89	177.72	-9.95
2180ps	18.20	1.30	108.01	161.90	-129.11	1.76	1.70	-15.80	2.15	172.41	23.30
5344ps	14.30	1.37	106.70	148.40	-147.00	1.77	1.64	41.20	1.88	175.54	-75.01
3984ps	25.90	1.41	114.73	85.93	-137.36	1.65	1.62	-36.40	1.88	166.25	-47.10

Table S2 Geometric parameters of Transition State. Distances are presented in [Å], angles and torsion angles in [º].

Structure	$\Delta E^{\#}$	Distance δ_1	Torsion Angle φ_1	Torsion Angle φ_2	Distance δ_3	Distance δ_3	Torsion Angle φ_3	Distance δ_2	Angle α_2	Torsion Angle φ_3
SBMD	19.00	3.12	179.26	179.19	1.63	1.69	-68.49	1.79	174.28	-107.44
4960ps	16.40	3.12	179.36	-178.74	1.70	1.64	-74.18	1.87	160.77	-100.76
2180ps	18.20	2.69	-174.10	-167.70	1.75	1.70	-38.24	1.84	172.05	18.54
5344ps	14.30	3.20	173.96	-177.24	1.77	1.65	-71.72	1.88	160.34	-107.49
3984ps	25.90	3.62	177.17	174.35	1.65	1.63	-65.48	1.78	165.51	-74.19

Table S3 Geometric parameters of Product Complex. Distances are presented in [Å], angles and torsion angles in [º].

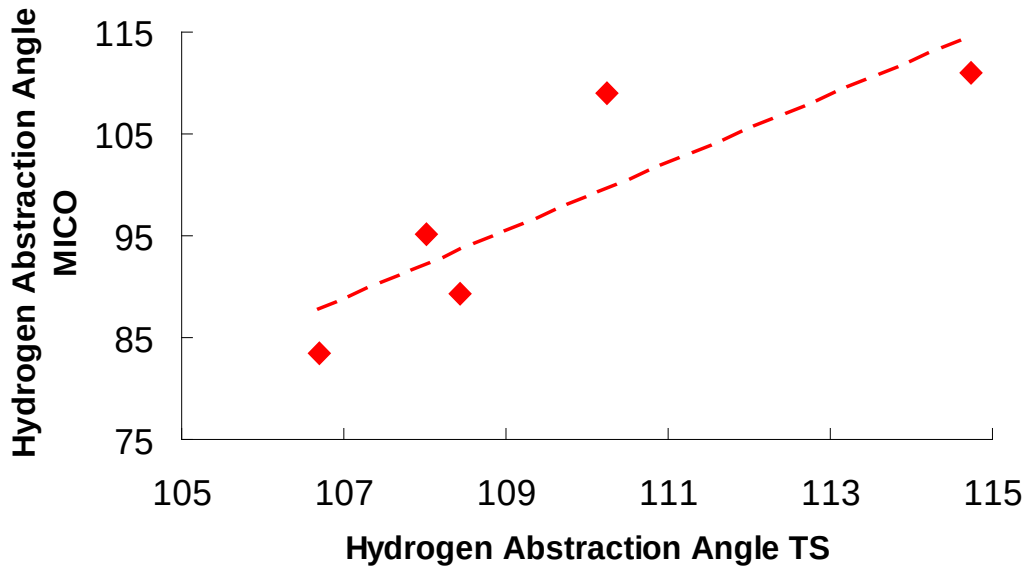

Figure S3. Correlation between hydrogen abstraction angle in the Michaelis complex and the transition state